Physical-controlled CO_2 effluxes from reservoir surface in the upper Mekong River Basin: a case study in the Gongguoqiao Reservoir

Lin Lin[1], Xixi Lu[1, 2, *], Shaoda Liu[3], Shie-Yui Liong[4] and Kaidao Fu[5, *]

[1]Department of geography, National University of Singapore, 117570, Singapore
[2]Inner Mongolia Key Lab of River and Lake Ecology, School of Ecology and Environment, Inner Mongolia University, Hohhot, Inner Mongolia, 010021, China
[3]Yale School of Forestry & Environmental Studies 195 Prospect Street New Haven, CT 06511. USA
[4]Tropical Marine Science Institute (TMSI), National University of Singapore, 117570, Singapore
[4]Asian International River Center, Yunnan University, Chenggong University City, Chenggong, Kunming, Yunnan, 650500, China

Correspondence to: Kaidao Fu(kdfu@ynu.edu.cn)

Abstract. Impounding greatly alters the carbon transportation in rivers. To quantify this effect, we measured CO_2 effluxes from a mountainous valley-type reservoir in the upper Mekong River (Lancang River in China) and compared them with those from the river channel. Evasion rates from the reservoir surface were 408±337mg m^{-2} d^{-1} and 308±261mg m^{-2} d^{-1} in the dry season and the rainy season respectively, much lower than those from riverine channel of 2168±2567mg m^{-2} d^{-1} and 364±195mg m^{-2} d^{-1}at the mainstem and the tributary respectively. Low effluxes in pelagic area resulted from few allochthonous organic carbon (OC) inputs and photosynthetic uptake of CO_2. The negative relation between efflux and water temperature suggests that CO_2 emissions at the pelagic area were partly offset by photosynthesis in the warmer rainy season. The emissions from the reservoir outlet and the littoral area, which were usually considered as hotspots of CO_2 emissions, contributed little to the total emission because of epilimnion water spilling and small area of littoral zones. Yet the higher effluxes were recorded at the river inlets in the dry season when the inflow and outflow were small because of different mixing modes occurring in the two seasons. When the river joined the receiving waterbody in the dry season, the warmer, clear and lighter inflow became an overflow and substantial CO_2were released to the atmosphere as the overflow contacted the atmosphere directly. Extended water retention time due to water storage might also help mineralization of OC. In the wet season, however, the colder, turbid and heavier inflow plunged into the reservoir and was discharged to the downstream with carbon for hydroelectricity, leaving insufficient time for decomposition of OC. Besides, diurnal efflux variability indicated that the effluxes were significantly higher in the night than in the daytime, which increased the annual emission rate by a half.

1 Introduction

Supersaturation of CO_2 in the inland waters (Cole et al., 1994) results in substantial carbon outgassing to the atmosphere annually (Battin et al., 2009; Cole et al., 2007; Raymond et al., 2013; Tranvik et al., 2009). Loss of carbon to the atmosphere from inland waters has been recognized as an important part of carbon cycling which faces great anthropogenic impacts (Maavara et al., 2017; Regnier et al., 2013). Damming rivers to build large reservoirs for water supply, irrigation, hydroelectricity and flood controls is one of the most drastic changes in inland waters (Lehner & Döll, 2004; Varis et al., 2012; Yang & Lu, 2014). By flooding large area of forests, soils and different kinds of organic matter, reservoirs have been identified as a large potential carbon source to the atmosphere since last century and have caused a serious perturbation on the global carbon budget (Fearnside, 1997; Kelly et al., 1994; Rudd et al., 1993). Damming rivers not only enlarges the water surface, but also produces more greenhouse gases (GHGs), mainly carbon dioxide and methane, than the natural waterbodies (Barros et al., 2011, Deemer et al., 2016, Mendonça et al., 2012a). Most of the carbon is released in the form of carbon dioxide, even though methane takes up the majority of the GHG emissions (calculated with CO2 equivalents) due to its high global warming potential (GWP) (Deemer et al., 2016, Demarty and Bastien, 2011).

Efforts have been made to evaluate CO_2 emissions from reservoir surfaces (Raymond et al., 2013; Varis et al., 2012; Vincent et al., 2000) and the accumulated case studies indicate that CO_2 emission rates exhibit great seasonal variability and spatial heterogeneity (Barros et al., 2011; Deemer et al., 2016). Quantity and quality of DOC and water temperature are considered as the most important factors that control the CO_2 fluxes from reservoirs as young tropical reservoirs and those with substantial labile OC tend to have higher emission rates (Barros et al., 2011; Mendonça et al., 2012a; Tadonleke et al., 2012). However, in China, the country with the most dams in the world (Yang et al., 2016), analysis on pCO_2 shows that most of the effluxes from reservoir surface were much lower than that from tropical and boreal reservoirs (Li & Zhang, 2014; Li et al, 2015; Liu et al., 2016b; Ran et al., 2017). Lower effluxes in the reservoir center (Gao et al., 2017; Mei et al., 2011; Liu et al., 2016b; Liu et al., 2017) imply that the pCO_2 in reservoir surface is subject to photosynthetic uptake of phytoplankton (Ran et al., 2017; Ran et al., 2018). The pCO_2 and effluxes from reservoirs are regulated by the balance between respiration and photosynthesis and quite sensitive to the monsoon climate due to the seasonal variation of water temperature and hydrological condition (Guo et al., 2011; Mei et al., 2011). For example, in the Three Gorges Reservoir, one of the largest reservoirs in China, CO_2 emissions from the littoral zone are subjected to the seasonal flooding (Chen et al., 2009; Yang et al., 2012) and the carbon uptake of algae in the stagnant tributaries resulted from heavy eutrophication, was heavily influenced by the seasonal variation of hydrological condition(Jiang et al., 2012, Guo et al., 2011, Ran et al., 2011, Zhao et al., 2013)

Despite the spatial heterogeneity (Li & Zhang, 2014), the research reviewed above mostly focused on the reservoirs in the highly populated eastern plain where the waterbodies are suffering from heavy eutrophication (Li & Zhang, 2014; Mei et al., 2011). In the less populated southwestern China where two-thirds of the exploitable hydropower were found and many more reservoirs are being built, however, the dynamics underlying CO_2 emissions has been less understood (Hu & Cheng, 2013). Rivers originate from the Tibetan Plateau and flow through the mountainous area of Southwestern China, receiving flows from melted glaciers and rainfalls brought by the South Asian monsoon. The precipitation in summer and autumn account for 50% and 27% of the annual rainfalls respectively, producing high waterflow in the warm rainy season. It was supposed that the CO_2 emissions of these rivers are more sensitive to the monsoon climate which regulates rainfalls, nutrient availability, and water discharge. However, the river flows are also regulated by the dams. In particular, dams completed upon the upper basin of Mekong River (or the Lancang River), one of the most important rivers in Southeast Asia, have largely affected the hydrological condition, sediment transportation and the CO_2 emissions (Lu and Siew, 2006; Lu et al., 2014).

In this study, the Gongguoqiao Reservoir (GGQ), the uppermost reservoir in the Lancang cascading reservoir, was selected as a site for the investigation of the seasonal variation of the dynamics of carbon effluxes in these reservoirs. This research aimed to measure the CO_2 evasion with static chamber method and analyze the spatial heterogeneity, seasonal variation and diurnal variation of the CO_2 efflux, in order to examine the mechanism that controls the CO_2 effluxes under the monsoon climate and the damming effect on carbon emissions. Considering there are seven completed dams on the upper Mekong Basin and another fourteen dams are either under construction or planned, clarifying the coupling effect of the climatic and damming effect on the CO_2 emissions can help understand the role of inland waters in the global carbon cycle.

2 Methods

2.1 Study area

The Gongguoqiao Reservoir (GGQ) is located in Gongguo Town (Fig. 1, 25º35’9.87”N, 99º20’5.55”E) in Dali Prefecture (Yunnan, China).With a catchment area of 97,200 km^2, around 32 billion m^3 of water flow into the reservoir annually. The monthly water discharge of inflow to the GGQ Reservoir in 2016 is shown in Fig. 2. Point L (Jiuzhou) is considered the point dividing the upper and middle reach of the Lancang River (Fig. 1). The area is subject to a subtropical monsoon climate where over 80% of the annual rainfallsbring78.6% of the annual water discharge and 95% of the annual sediments loads to the reservoir in the rainy season spanning from May to October(Fig.2,He and Tang, 2000).The annual precipitation is 804.90mm and the monthly air temperature ranged from 7.6 ℃ to 21.6 ℃, with an average of 17.8 ℃ (Fig. S1, Hu, 2010). There are several villages scattered along the riverside. Before the reservoir filling, the average vegetation covered25% of the steep slope but the vegetation keeps degrading due to intense agricultural activities (Hu, 2010, Xu et al., 2003). The reservoir was filled in Sep 2011 and had been the uppermost cascading reservoir in the upper Mekong River Basin until the end of 2016 when the Miaowei Reservoir was filled at its upstream. The outflow from GGQ feeds the Xiaowan Reservoir at the downstream. The backwater area stretches 44.3 km along the mainstem and 7 km along the tributary, the Bijiang River respectively. The width of the reservoir ranges from 110m to 120m in the dry season. The standard water level is 1307m, corresponding to a storage of 0.316 billion m^3. The reservoir uses epilimnion water (around 4~5m deep) for hydropower production and generates 4.041 billion kW/h annually. The reservoir is a daily-operated reservoir due to its small operating capacity (49 million m^3). Thus, the water level fluctuates frequently and the average water retention time is 1.4 days. Water column is well mixed in the deep pelagic area (depth>5m) from May to August while stratified in the rest of the year (unpublished data in this research).

2.2 Study methods

2.2.1 Sampling

Five sampling points were selected along the mainstem and two from the Bijiang River, a turbid tributary joining the reservoir about 1km before the dam (Fig. 1). The sampling points where the surface velocity could be detected (v>0m/s) were defined as river channels. The average flow velocity was 0.2m/s and 0.7m/s at Point R1 and R2 respectively. Thus these points were considered as river channels and the flows in channels were regarded as the inflows to the reservoir. Even though the Miaowei Reservoir under construction during the sampling period might have affected the deposition processes of the river, since the water was not impounded and regulated by the dam, Point R1 was considered as pristine river channel. Another point was selected for comparison at the downstream of the dam (Point D) where the flow was regarded as outflow. The flow velocities at all the other points were zero, indicating that the points are in the reservoir. Among the points in the reservoir, Points P1~P4 were defined as pelagic points as they were permanently flooded. Point L was defined as littoral zone with daily flooding and draining owing to the frequent fluctuation of the water levels. The point was on a wetland formed by fine sediments deposited on a relatively flat platform.

The sampling campaign started in January 2016. The first two campaigns were carried out in January and March. Samples were collected only in riverine channels, including Point R1, R2 and D. The formal campaigns were conducted twice a month from April to December 2016 before the impounding of the Miaowei Reservoir at the upstream. Samples were collected from 9am to 4pm when sunlight was available and each campaign lasted two to three days. The emission rates were measured following the same order among sampling points, yet we failed to collect the samples at the Point L in late October as it dried out due to a low water level. Totally 127 samples were collected in 16 formal campaigns. For the diurnal variation in fluxes, discontinuous samplings were completed in the riverine sites during the first sampling campaign in January while the continuous diel sampling on CO_2 effluxes was conducted at a permanently flooded point adjacent to Point L before the last sampling campaign.

The effluxes were measured in situ with a floating chamber connected to a non-dispersive infrared CO_2analyzer (S157-P 0-2000ppm, Qubit, Canada) via the LQ-MINI interface (Vernier, USA). The chamber is a 20cm x 12cm x 10cm polypropylene rectangle translucent box inserted through a diamond-shape Styrofoam collar. It was turned upside down three times to mix the gas within the box. The CO_2 analyzer could detect the partial pressure of CO_2 down to 1ppm and it was calibrated before the sampling campaigns started. The Measurement of CO_2 concentration did not begin until the reading of the analyzer became stable at around 400~500ppm. The chamber was fixed to the piles while floating on the water surface.

Calculation of effluxes was based on the slope of graph of concentration versus time according to methodology proposed by Tremblay et al. (2005). The equation was listed as Eq. 1:

$$Efflux = \frac{slope \times volume}{surface}, \quad (1)$$

In the equation above, *volume* refers to the air trapped in the chamber and *surface* refers to the surface of the floating chamber over the water. The *slope* was calculated with the variation curve of pCO_2. The emission pulses were excluded, and the slope was accepted only when the fitting curve had a R^2 higher than 0.90. Water temperature, pH, conductivity and dissolved oxygen (DO) were measured in situ with a portable multiparameter meter (Orion Star A321, Thermo Scientific, USA) with a resolution of 0.1℃, 0.01, 0.01μS/cm and 0.01mg/L, respectively. All the probes were calibrated before each sampling campaign started according to the manual. Due to malfunction of the instrument, the DO data was not available since September. Air temperature and wind velocity were measured with a portable anemometer (GM8901, Benetech, China). All the parameters were measured three times to reduce systematic error. For quality control, at least three water samples were collected from 0.5m below the water surface with water bottles. For alkalinity, the water samples were titrated with 2M hydrochloric acid within 12 hours after collection. The acid solution was titrated with NaOH solution. The alkalinity, pH and water temperature were used to calculate the partial pressure of CO_2 (pCO_2) with CO2SYS program (Lewis et al., 1998). The water samples were stored in 50ml centrifugal tubes and transported to the lab at a low temperature.

2.2.2 Laboratory analysis

The water samples for analysis of chlorophyll concentration were filtered with qualitative filter paper (80~120 μm) while the water samples for DOC analysis were filtered with 0.7μm Whatman GF/F filters to remove the sediments. Concentration of chlorophyll was analyzed with a Phyto-PAM-II Multiple Excitation Wavelength Phytoplankton analyzer (Heinz Walz GmbH, Germany). The DOC analysis was conducted on the Vario TOC Analyzer (Elementar, Germany). The resolutions of the analyser for chlorophyll and DOC are0.01 μg/L and 0.001ppm respectively. Unfiltered water samples were analyzed with spectrophotometer (UV5500, Metash, China) after digestion with alkaline potassium persulfate and potassium persulfate for concentration of total nitrogen (TN) and total phosphorous (TP) according to HJ636-2012 (MEP, 2012) and GB11893-89 (MEP, 1989) respectively.

3 Results

3.1 Spatial and temporal variation of environmental factors

Seasonal variations of temperature and rainfall reflect the characteristics of monsoon climate (Fig.S1). In winter (from December to February), the air temperature was below 5 ºC while the monthly average temperature was all over 25 ºC in summer (from June to August). The peak discharges of inflows in mainstem and tributary were both recorded in July, which were $70.50*10^8m^3$ and $4.02*10^8m^3$. The inflows in summer accounted 47% and 65% of the annual discharge in mainstem and tributary respectively. The water in the inflow was characterized by low temperature, pH, nutrient concentration and high alkalinity, conductivity, DOC concentration and chlorophyll, while the pelagic zone was filled with warm, more alkaline, eutrophic, but less aerobic water (Table 1). The water temperature ranged from 15.6 to 17.4 ºC, with an average of 16.8 ºC. The difference in water temperature between riverine zone and pelagic zone was no more than 2℃. Since the epilimnion water was used for hydropower generation, the water temperature in the downstream of the dam was very close to the surface water upstream of the dam. The pH values were mostly higher than 8.0 (averagely8.46), which suggested that the water in the reservoir was alkaline without any significant spatial heterogeneity. Total alkalinity ranged from 2251 μmol/L to 2666 μmol/L, with a mean value of 2441 μmol/L. Points located in the upstream had higher alkalinity than the downstream pelagic area with the maximum recorded in the littoral zone. Ranging from 345 μS/cm to 388 μS/cm, conductivity showed a similar variation trend as the alkalinity. The dissolved oxygen concentration in the pristine channel was approximately 4 mg/L higher than that in the pelagic area. Concentration of DOC was also significantly higher in the riverine zone than in pelagic area, but it was quite homogeneous within the reservoir, possibly due to severe deposition. Both the concentration of TN and TP showed low values in the reservoir, with a mean value of 0.71 mg/L and 0.15 mg/L respectively. The maximum concentration of nutrients was found in the littoral zones and pelagic area rather than in the riverine area on the mainstem.

3.2 Spatial and seasonal variation of pCO_2

Most of the water samples had pCO_2 higher than the atmospheric value (410 μatm) and supersaturated with CO_2 (Table 1 & Fig. 3), suggesting that the reservoir was a CO_2 source to the atmosphere. The partial pressures recorded in this study ranged from 237 μatm to 14764 μatm, with an annual average of 919 μatm and a median of 711 μatm. The values were close to the global average of artificial reservoirs (Raymond et al., 2013).

The annual pCO_2 of the reservoir (703 ± 407 μatm) was comparable to the natural lakes in the Yunnan-Guizhou Plateau (639 μatm, Wang et al., 2003) when the pCO_2 from the river channel was excluded. The results were much lower than the pCO_2 of Lower Mekong River (Li et al., 2013). Although there were no data available from the origin of the Mekong River, the research on the three rivers on the Tibetan Plateau showed a median pCO_2 of 864 μatm, which was comparable to the values in the GGQ (Qu et al., 2017).

The $pCO_2$was 852 ± 1056 µatm and 733 ± 232 µatm in the inflow of mainstem and the tributary respectively. These values were a little higher than the pCO_2 in the surface water of the pelagic zone, but the difference was insignificant ($p>0.05$). Since the pH was higher than 8 and varied little, the pCO_2 showed no significant spatial heterogeneity in the reservoir in spring, summer and winter. The pCO_2 was below 800 µatm from May to August while it increased drastically in late August. From September to April, the water level gradually rose and the pCO_2 fluctuated between 400 µatm and 1,200 µatm.

However, variation of the pCO_2 was significant ($p<0.05$) among four seasons as the pCO_2in autumn was much higher than in the other seasons. When the pCO_2 in the riverine area and the pelagic zone recorded their peak values in autumn, a significant decreasing trend toward downstream was found along the mainstem, which could be related to low pH at the reach from R1 to L ($p<0.05$) (Fig. 3). Frequent fluctuation of the water level and continued rainfalls flushed plenty of deadwood and organic matter to the reservoirs. Decomposition of the deadwood and plants could acidify the water along the bankside, which finally led to much higher pCO_2 in R1, P1 and L. Accumulation of deadwood was most obvious in the littoral zone because this area was flat for deposition. The pCO_2 in the littoral zone was 14764 µatm and 11825 µatm in September and October respectively. The extremely high pCO_2 in the littoral zone indicated that this zone could be a potential "hotspot" for carbon emissions.

The pCO_2 measured at the downstream of the dam was quite stable throughout the year ($p>0.50$), with an average of 658 ± 176 µatm. No drastic increase from P3 to D was found throughout the year. The gradient in pCO_2 between P3, the point close to the dam, and D, at the downstream of the dam, ranged from -247 µatm to 560 µatm. The pCO_2 was found to be lower at the downstream of the dam than upstream from August to November. Unlike the cascade reservoirs on the Maotiao River where a higher pCO_2 at the downstream of the dam had been consistently recorded (Wang et al., 2011), the pCO_2 at the downstream of GGQ rarely reached 10,000 µatm.

3.3 Spatial and seasonal variation of CO_2 effluxes

Fig. 4 and Fig. 5 showed the CO_2 effluxes displayed large spatial and seasonal variation in GGQ ($p<0.01$). The CO_2 effluxes ranged from -44 to 4952 mg m^{-2} d^{-1}averaged for the whole reservoir, with a mean value of 352 mg m^{-2} d^{-1}, or 8 mmol m^{-2} d^{-1}. Only one negative value suggesting carbon absorption was found in P4. It confirmed that the reservoir was a carbon source to the atmosphere, but the result was much lower than the estimated global average (Deemer et al., 2016; Holgerson & Raymond, 2016; Vincent et al., 2000). The annual effluxes at P1, P2, P3 and P4 were 465 ± 529mg m^{-2} d^{-1}, 331 ± 94 mg m^{-2} d^{-1}, 336 ± 92mg m^{-2} d^{-1} and 273 ± 11mg m^{-2} d^{-1}respectively. Effluxes in the pelagic zone were lower in summer and autumn than in winter and spring but the seasonal variation was not significant ($p>0.50$).

Fig. 5 displayed a decreasing trend of CO_2 efflux toward downstream. The annual efflux from the river channel was 1577mg m^{-2} d^{-1} and 905mg m^{-2} d^{-1} in mainstem and tributary respectively, which was significantly higher than that in reservoir area ($p<0.50$). The efflux in R1 was very sensitive to the monsoon climate. During summer, the efflux in R1 was no more than 274mg m^{-2} d^{-1} but it rapidly climbed to 2359 mg m^{-2} d^{-1} at the end of October. The efflux stayed above 6,000 mg m^{-2} d^{-1} in the winter and the high rate persisted till the following March. Hence, the difference in efflux between river and reservoir was more significant in the dry season than in the wet season.

The average efflux at Point D at the downstream of the dam was similar to that of Point P3 (341 ± 158 mg m^{-2} d^{-1}), aligned with the results of pCO_2 (Table 1 & Fig. 3). The emission at the downstream was higher in summer and winter, while it dropped below 300 mg m^{-2} d^{-1} in spring and oscillated between 200 and 300 mg m^{-2} d^{-1} in autumn. The low values contradicted the findings for many tropical reservoirs (Abril et al., 2005; Chanudet et al., 2011), but was consistent with the low pCO_2reported for some mountainous reservoirs in eastern China (Zhao et al., 2013). The areal efflux downstream of the dam was consistently lower than that from the epilimnion in the reservoir because degassing could occur when the water passed through the turbine for electricity generation. It suggested that the carbon emission rate downstream of the dam was determined by the position of the water inlet and source layer of the water passing through the turbine.

The littoral zone had the highest emission rates within the reservoir (684 ± 1153mg m^{-2} d^{-1}), although this value was less than one third of the efflux estimated for drawdown areas in temperate reservoirs (Aufdenkampe et al., 2011; Li et al., 2015). This was mainly because of the higher pCO_2. In autumn the littoral zone had the highest $pCO_2$and the highest efflux along the reservoir when the frequent water level fluctuated widely.

3.4 Diurnal variation of CO_2 effluxes

In GGQ the effluxes showed significant difference between daytime and nighttime ($p<0.01$). The diurnal observation of effluxes in the littoral zone showed that the CO_2 efflux was two times higher at night (from 19:00 to 7:00: averagely 495 ± 178 mg m^{-2} d^{-1}) than in the daytime (from 7:00 to 19:00: averagely 247 ± 171 mg m^{-2} d^{-1}) (Fig. 6 & Fig. 7). The CO_2 efflux was two times higher at night (from 19:00 to 7:00: 495 ± 178 mg m^{-2} d^{-1} on average) than in the daytime (from 7:00 to 19:00: averagely 247 ± 171 mg m^{-2} d^{-1}). The trend was verified by the discontinuous efflux measurements in which the nocturnal CO_2 flux (1012.29 ± 1016.84 mg m^{-2} d^{-1}) was higher than the daytime flux (766.87 ± 740.43 mg m^{-2} d^{-1}). The efflux was negatively related to air temperature, wind speed and pH, but positively related to conductivity, alkalinity and pCO_2 ($N=40$, $p<0.01$). Thus higher efflux at night was resulted from dominated respiration in the surface water when light was unavailable for photosynthesis, which was also commonly found in other reservoirs (Liu et al., 2016a; Peng et al., 2012; Schelker et al., 2016).

Fig. 6 shows that pCO_2 was higher with an average of 969 μatm at night, but lower with an average of 871 μatm in the daytime. However, there was drastic oscillation of efflux from 9pm to 11pm with a range spanning from 712 mg m^{-2} d^{-1} to 69 mg m^{-2} d^{-1}. Before 8pm, the efflux was kept below 400 mg m^{-2} d^{-1} but rose to above 450mg m^{-2} d^{-1} after 0:30 at midnight. Statistically there was no significant difference in pCO_2 between nighttime and daytime ($p>0.50$).

The diurnal variation in pCO_2 was also insignificant because the pH varied little within a daily circle ($p>0.50$). The pH was 8.21 on the average with a range of no more than 0.28. However, a slight decrease in pH was found at night, which led to an increase of pCO_2 and efflux. The water temperature increased from 13:00 to 19:30 but kept decreasing after 22:00. As the air temperature kept decreasing throughout the sampling period, the water was heated before 24:00 and started to lose heat to the atmosphere afterwards. The alkalinity dropped from 15:00 to 19:30 and increased since 20:00. With a mean value of 2904 μg/L, alkalinity reflected a similar variation trend as pCO_2. Like the pH, the conductivity also varied little with the value ranging from 527.7 μS/cm to 540.8 μS/cm. The wind speed was higher in the daytime; the maximum (3.5m/s) was recorded at 16:30, while in the nighttime the sampling point was dominated by calm wind conditions.

4 Discussion

4.1 Damming effect on carbon effluxes in the Upper Mekong River

In this study, the CO_2 emission rates of the four-year old reservoir were comparable to those of natural lakes (Xing et al., 2005, Wang et al., 2003). Even in the river channel, the highest effluxes were close to the effluxes from temperate reservoirs (Huttunen et al., 2002) and much lower than those from tropical reservoirs (Abril et al., 2005; Fearnside, 1997; Guérin et al., 2006). There are multiple reasons for the low carbon effluxes. First, the upper Mekong River drains through the Tibetan Plateau and within a narrow valley before it reaches the GGQ. Because of poor vegetation in the catchment and intense precipitation during the rainy season, the catchment cannot sustain fertile soil or provide abundant organic carbon for decomposition even in the wet seasons. A shortage of substrates for mineralization limits the production of carbon dioxide.

Secondly, damming the river greatly extends the water retention time and the riverine ecosystem gradually evolves into a limnetic ecosystem (Thornton et al., 1990). The extended water retention time in the pelagic zone of reservoirs is suitable for the development of phytoplankton communities. When light and temperature are favourable, intense photosynthesis consumes the CO_2 dissolved in surface water and lower the emission rates (Yu et al., 2009). In extreme cases like algae bloom, the surface water tends to absorb CO_2 from the atmosphere (Pacheco et al., 2014b). Thus, the valley-type reservoir exhibited a decreasing trend from the river towards the dam in pCO_2 and the outgassing rates (Liu et al., 2009; Liu et al., 2014; Mei et al., 2011). Anthropogenic nutrient input can accelerate the process of eutrophication. With abundant nitrogen and phosphorous input from sewage, the outgassing rates could be decreased to a level as low as natural lake or even turns negative (Guo et al., 2011; Ran et al., 2011). The effluxes from the GGQ displayed a negative relation with the water temperature ($p<0.01$, Fig. 8). The negative relation deviated from the traditional pattern where a warmer climate accelerated bacterial respiration (Åberg et al., 2010; Del Giorgio & Williams, 2005) and decreased the solubility of carbon dioxide, thus enhancing the effluxes. This deviation suggests that warmer climate could also reduce the CO_2 emissions via accelerated photosynthesis.

The seasonal difference in the pelagic area, however, was less significant ($p>0.05$) than the variation in the riverine sites of Point R1 and R2 ($p<0.01$). The riverine inlets of the reservoir were identified as a hotspot of CO_2 emission in the dry season (from November to April), where the extremely high emission rates distinguished from the emission from pelagic area ($p<0.01$). In some large valley-type reservoirs rainfalls bring plenty of organic carbon and increase flow velocity, fuelling CO_2 emissions at the mainstem channels in the wet season (Li & Zhang, 2014; Zhao et al., 2013). Yet in this case the efflux at the riverine points were negatively related to the water discharge (Fig. 9), water temperature, and nutrient concentration (Table S1), suggesting that higher emissions could happen at a lower flow velocity and a colder condition (Fig. 8&9).

This abnormal results could be explained by different mixing modes occurring at the riverine points when the inflow joined the reservoir, which can be represented by the differences in physical properties like temperature and turbidity (Summerfield, 1991).As shown in Fig. 10, the inlets had higher effluxes when the gradient in temperature and suspended sediment concentration between the inflow water and the reservoir surface water was larger. It suggests that the seasonal variation of effluxes was regulated by both flow mixing modes and reservoir management (Striegl & Michmerhuizen, 1998). Even though in the rainy season intense precipitation could bring plenty of sediments with organic matter, the turbid water might be discharged directly to the downstream for electricity, because of the relatively small storage capacity of the reservoir. The inflow water with high sediment concentration is heavier and colder than the reservoir water, thus it plunges into the water column in the reservoir and becomes an underflow (hyperpycnal flow, Fig. 10) (Summerfield, 1991). The reservoir surface is less affected by the underflow and maintained a relatively low emission rate (Pacheco et al., 2014a) as continuous water discharging allows little time for the mineralization of organic carbon (Assireu et al., 2011; Senturk, 1994), in spite of the high flow velocity. However, in the dry season, the clean inflow water is lighter and warmer than the reservoir water, and thus it joins the reservoir as surface flow (hypopycnal flow, Fig. 10) (Summerfield, 1991). The data in Fig. 3 shows that the inflow water in the winter (the dry season) was also richer in CO_2 than the turbid inflow in the summer (the wet season). When the water rich in CO_2 contacts the atmosphere directly, the gases directly diffuse into the air. Because the water keeps losing CO_2 to the atmosphere, the decreasing trend in effluxes towards downstream is more significant in winter (Fig. 5).

Due to this difference in physical mixing modes and availability of CO_2, the surface water tended to release more CO_2 in the dry season when both inflow and reservoir water became colder (Fig. 4). It was likely that the underflow in the rainy season also mixed and aerated the water in the reservoir and thus impeded the formation of stratification. The efflux in the downstream was restricted and showed a similar seasonal variation to the reservoir surface water since during stratification water from anoxic hypolimnion is rich in carbon dioxide and is likely to release large amount of carbon dioxide when it passes the turbine, leading to intense emissions at the downstream river channel (Abril et al., 2005; Guérin et al., 2006; Wang et al., 2011).

The littoral zone (or drawdown area) displayed much higher effluxes than the pelagic zone, especially in autumn and winter. The littoral zone had often been identified as a hotspot of carbon emission (Chen et al., 2009; Yang et al., 2012; Yang, 2011) since seasonal flooding could trigger anaerobic decomposition of dead macrophytes and produced greenhouse gases. In this case, it is believed that the frequent fluctuation of water level deposited a large amount of sediments as well as deadwood on the relatively flat littoral zones. The decomposition of deadwood tended to release organic acids to the water and lowered the pH. As a result, the pCO_2 rose and more gases were degassed out of the air-water interface. Furthermore, nutrients input and reduced turbidity facilitated growth of plants and macrophytes (Thornton et al., 1990) and enhanced respiration and CO_2 outgassing (Fig. S2, Xu, 2013).

4.2 Extrapolation of the results and implication for future studies

The efflux from the pelagic zone and from the littoral zone was 352 mg m^{-2} d^{-1} and 684 mg m^{-2} d^{-1} respectively. Assuming the water level fluctuated frequently within 2.5m and the slope at the bank was 45º, the drawdown area covered an area of $1.81 \times 10^5 m^2$. Hence the littoral zone could contribute 6.16t of carbon to the atmosphere, assuming it would be flooded in half of the year. We estimate that the permanent flooded area will be 5,643,000m^2 for the GGQ. The carbon dioxide evading from this area will be 200t annually. Compared with the emission rate, the contribution from the littoral zone is actually negligible for its small area. However, if one takes the diurnal variation into account, the annual carbon evasion will reach 300t as nocturnal effluxes was twice as the emission in daytime. Considering its efficiency, the reservoir releases 0.28 kg CO2 per MW/h when generating hydroelelctricity. This estimation is close to the lower bound of the range (0.2~1994kg CO_2 per MW/h) estimated by Räsänen et al. (2018). However, it must be noted that the CO_2 efflux will decrease as the reservoir ages (Abril et al., 2005; Barros et al., 2011). Accelerated eutrophication could possibly fix more CO_2 via photosynthesis (Liu et al., 2009).

Several problems have been noticed when computing the annual emission rate from the GGQ. Despite its higher efflux, the drawdown area is negligible although the effluxes from global reservoirs always displayed high spatial heterogeneity (Barros et al., 2011; Roland et al., 2010; Teodoru et al., 2011). On a larger scale the seasonal variation is also negligible as the efflux in the dry season was only 103 mg m^{-2} d^{-1} higher than in the rainy season. At the same time, the higher effluxes in the nighttime must be taken into consideration. Measurement of the effluxes from the reservoir surface is usually limited by the pCO_2samples collected in the daytime and fails to capture a diurnal variation, though this variation has been fully recognized by a series of studies (Liu et al., 2016a; Peng et al., 2012; Schelker et al., 2016).

The sediment deposition must also be considered when computing the long-term effect of reservoir on carbon cycle. As the uppermost reservoir along the Lancang cascades, GGQ also sequestered most of the sediments from the upstream catchments (Gao et al., 2017; Wang et al., 2011). It is likely that the reservoir cannot be maintained for 100 years due to heavy silting problem (Fu & He, 2007), even though the sediment concentration has decreased drastically after the upstream Miaowei Dam was completed, enabling the reservoir to bury tons of organic carbon (Mendonça et al., 2012b; Mulholland & Elwood, 1982; Vörösmarty et al., 2003). Meanwhile the reservoirs could also sequester the nutrients in the rivers (Maavara et al., 2017; Maavara et al., 2015). Therefore, in order to evaluate the net effect of impoundments on carbon cycle, we need to quantify the organic carbon burial within the reservoir and finally build up a robust carbon budget.

5 Conclusion

The surface water of the GGQ was supersaturated with CO_2 and the reservoir was a carbon source to the atmosphere. We estimate that the reservoir releases 3.0 tons of CO_2 to the atmosphere annually. The efflux from reservoir area was 408 mg m^{-2} d^{-1} and 305 mg m^{-2} d^{-1} in the dry season and rainy season respectively, while the river channel exhibited an efflux of 2168 mg m^{-2} d^{-1} and 374 mg m^{-2} d^{-1} in the two seasons. The CO_2 emission from pelagic zone was limited due to few allochthonous organic carbon input and photosynthetic uptake owing to extended water retention time. Seasonal variation of efflux in the reservoir was subject to the variation of temperature, with lower emission rates occurring in the warmer wet season (May to October) owing to enhanced photosynthesis. Emissions at downstream of the dam was also limited as surface water was used for generating electricity. However, the littoral zone suffering frequent flooding and draining was identified as a potential hotspot of CO_2 emissions, even though its contribution to the total annual emission was limited for its small area. Flat topography and daily flooding could lead to accumulation of deadwood and acidification of water, aerate the water and enhance the respiration rate.

This study also highlights the high emission rates at river inlets during the colder dry season. The negative relation between efflux and water discharge implies that the mixing modes could be the dominant factor controlling CO_2 emissions. In the winter, because inflow was warmer, clearer and lighter than the receiving waterbody, the gas carried by inflow could be more easily released to the atmosphere as the river joins the reservoir as an overflow. Additionally, extended water retention time was also beneficial for decomposition of allochthonous DOC and produced more carbon dioxide. In the wet season, when the inflow plunged into the reservoir, the unferflow could be discharged directly to the downstream and left insufficient time for the mineralization of OC. The physical factors could be an important factor controlling the CO_2 emissions beside the biological factors for hydroelectric reservoirs where the hydrological conditions are regulated by climate and artificial operation. Yet in a daily cycle, the biological factor could cause significant diel variation, as emissions could be offset by the carbon absorption via photosynthesis. The total emission from the GGQ increases by half when taking the nocturnal effluxes into account. Hence, the efflux measured in daytime must be carefully integrated when estimating the total carbon emissions from the reservoir. In this study, the damming effect on the CO2 emission from waterbody was moderate but for an overall effect on carbon transportation a robust carbon budget was required in which the carbon burial in sediments must also be quantified.

Acknowledgements

The research reported here has received funding from the National Natural Science Foundation of China (Grant No 91547110; 41571032) and financial support from National University of Singapore (Grant No. R-109-000-191-646; R-109-000-227-115).

References

Åberg, J., Jansson, M., & Jonsson, A.: Importance of water temperature and thermal stratification dynamics for temporal variation of surface water CO_2 in a boreal lake. Journal of Geophysical Research: Biogeosciences, 115(G2), n/a-n/a. doi:10.1029/2009JG001085, 2010.

Abril, G., Guérin, F., Richard, S., Delmas, R., Galy-Lacaux, C., Gosse, P., . . . Matvienko, B.: Carbon dioxide and methane emissions and the carbon budget of a 10-year old tropical reservoir (Petit Saut, French Guiana). Global biogeochemical cycles, 19(4), 2005.

Assireu, A., Alcântara, E., Novo, E., Roland, F., Pacheco, F., Stech, J., & Lorenzzetti, J.: Hydro-physical processes at the plunge point: an analysis using satellite and in situ data. Hydrology and Earth System Sciences, 15(12), 3689, 2011.

Aufdenkampe, A. K., Mayorga, E., Raymond, P. A., Melack, J. M., Doney, S. C., Alin, S. R., . . . Yoo, K.: Riverine coupling of biogeochemical cycles between land, oceans, and atmosphere. Frontiers in Ecology and the Environment, 9(1), 53-60, 2011.

Barros, N., Cole, J. J., Tranvik, L. J., Prairie, Y. T., Bastviken, D., Huszar, V. L., . . . Roland, F.: Carbon emission from hydroelectric reservoirs linked to reservoir age and latitude. Nature Geoscience, 4(9), 593-596, 2011.

Battin, T. J., Luyssaert, S., Kaplan, L. A., Aufdenkampe, A. K., Richter, A., & Tranvik, L. J.: The boundless carbon cycle. Nature Geoscience, 2(9), 598-600, 2009.

Chanudet, V., Desloux, S., Harby, A., Sundt, H., Hansen, B. H., Brakstad, O., Serca, D. & Guerin, F.: Gross CO2 and CH4 emissions from the Nam Ngum and Nam Leuk sub-tropical reservoirs in Lao PDR. Sci Total Environ, 409, 5382-91. 2011.

Chen, H., Wu, Y., Yuan, X., Gao, Y., Wu, N., & Zhu, D.: Methane emissions from newly created marshes in the drawdown area of the Three Gorges Reservoir. Journal of Geophysical Research - Atmospheres, 114(D18), D18301. doi:10.1029/2009JD012410, 2009.

Cole, J. J., Caraco, N. F., Kling, G. W., & Kratz, T. K.: Carbon dioxide supersaturation in the surface waters of lakes. Science, 265(5178), 1568-1570, 1994.

Cole, J. J., Prairie, Y. T., Caraco, N. F., McDowell, W. H., Tranvik, L. J., Striegl, R. G., . . . Middelburg, J. J.: Plumbing the global carbon cycle: integrating inland waters into the terrestrial carbon budget. Ecosystems, 10(1), 172-185, 2007.

Deemer, B. R., Harrison, J. A., Li, S., Beaulieu, J. J., DelSontro, T., Barros, N., . . . Vonk, J. A.: Greenhouse gas emissions from reservoir water surfaces: a new global synthesis. Bioscience, 66(11), 949-964, 2016.

Del Giorgio, P. A., & Williams, P. J. l. B.: Respiration in aquatic ecosystems: Oxford University Press, USA, 2005.

Demarty, M. & Bastien, J.: GHG emissions from hydroelectric reservoirs in tropical and equatorial regions: Review of 20 years of CH4 emission measurements. Energy Policy, 39, 4197-4206, 2011.

Fearnside, P. M.: Greenhouse-gas emissions from Amazonian hydroelectric reservoirs: The example of Brazil's Tucuruí Dam as compared to fossil fuel alternatives. Environmental conservation, 24(01), 64-75, 1997.

Fu, K., & He, D.: Analysis and prediction of sediment trapping efficiencies of the reservoirs in the mainstreamof the Lancang River. Chinese Science Bulletin, 52(2), 134-140, 2007.

Gao, Q., Tao, Z., Zhang, S., Xie, C., Lin, P., & Mao, H.: The Damming Effects on the Dynamics of Riverine Carbon in a Mountainous River: A Case Study in the Zengjiang River, South China. Quaternary Science, 37(2), 331-342, 2017.

Guérin, F., Abril, G., Richard, S., Burban, B., Reynouard, C., Seyler, P., & Delmas, R.: Methane and carbon dioxide emissions from tropical reservoirs: significance of downstream rivers. Geophysical Research Letters, 33(21), 2006.

Guo, J., Jiang, T., Li, Z., Chen, Y., & Sun, Z.: Analysis on partial pressure of CO_2 and influencing factors during spring phytoplankton bloom in the backwater area of Xiaojiang River in Three Gorges Reservoir. Advances in Water Science, 22(6), 829-838, 2011.

He, D. & Tang, Q.: Chinese International Rivers. Beijing, China: Science Press, 2000.

Holgerson, M. A., & Raymond, P. A.: Large contribution to inland water CO2 and CH4 emissions from very small ponds. Nature Geoscience, 9(3), 222. doi:10.1038/ngeo2654, 2016.

Hu, H.: Geological Hazard Risk Study of the Gongguoqiao Hydropower Station. Master, Lanzhou Univeristy, 2010.

Hu, Y. & Cheng, H.: The urgency of assessing the greenhouse gas budgets of hydroelectric reservoirs in China. Nature Climate Change, 3, 708-712, 2013.

Jiang, T., Guo, J., Li, Z., Fang, F., Bai, L. & Liu, J.: Air-Water Surface Greenhouse Gas Flux in Pengxi River at Different Operational Stages of the Three Gorges Reservoir. Environmental Science, 33, 1463-1470. 2012.

Kelly, C. A., Rudd, J. W., St Louis, V. L., & Moore, T.: Turning attention to reservoir surfaces, a neglected area in greenhouse studies. Eos, Transactions American Geophysical Union, 75(29), 332-333, 1994.

Lehner, B., & Döll, P.: Development and validation of a global database of lakes, reservoirs and wetlands. Journal of Hydrology, 296(1), 1-22, 2004.

Li, S.Y., Lu, X.,X.& Bush, R. T.: CO_2 partial pressure and CO_2 emission in the Lower Mekong River. Journal of Hydrology, 504, 40-56, 2013.

Li, S., & Zhang, Q.: Partial pressure of CO_2 and CO_2 emission in a monsoon-driven hydroelectric reservoir (Danjiangkou Reservoir), China. Ecological Engineering, 71, 401-414. 2014.

Li, S., Zhang, Q., Bush, R. T., & Sullivan, L. A.: Methane and CO_2 emissions from China's hydroelectric reservoirs: a new quantitative synthesis. Environmental Science and Pollution Research, 22(7), 5325-5339, 2015.

Liu, C., Wang, F., Wang, Y., & Wang, B. Response of Aquatic Environment to River Damming. Resources and Environment in the Yangtze Basin, 18(4), 384-396, 2009.

Liu, H., Zhang, Q., Katul, G. G., Cole, J. J., Chapin III, F. S., & MacIntyre, S.: Large CO2 effluxes at night and during synoptic weather events significantly contribute to CO2 emissions from a reservoir. Environmental Research Letters, 11(6), 064001. 2016a.

Liu, S.D., Lu XX, Xia XH, Zhang S.R, Ran L.S, Yang XK.: Dynamic. biogeochemical controls on river pCO2 and recent changes under aggravating river impoundment: an example of the subtropical Yangtze River. Global Biogeochemical Cycles, 2016b.

Liu S.D., XX Lu, X Xia, X Yang, L Ran.: Hydrological and geomorphological control on CO2 outgassing from low-gradient large rivers: An example of the Yangtze River system. Journal of hydrology 550, 26-41, 2017.

Liu, W., Pu, J.-b., Yu, S., Zhang, C., Au, Y.-y., Yuan, D.-x., . . . Tang, W.: Preliminary Research on the Feature of Dissolved Inorganic Carbon in Wulixia Reservoir in Summer, Guangxi, China (in Chinese). Environmental science, 35(8), 2959-2966, 2014.

Lu XX, S Li, M Kummu, R Padawangi, JJ Wang. Observed changes in the water flow at Chiang Saen in the lower Mekong: Impacts of Chinese dams?Quaternary International 336, 145-157, 2014.

Lu XX, RY Siew.: Water discharge and sediment flux changes over the past decades in the Lower Mekong River: possible impacts of the Chinese dams. Hydrology and Earth System Sciences Discussions 10 (2), 181-195, 2006.

Maavara, T., Lauerwald, R., Regnier, P., & Van Cappellen, P.: Global perturbation of organic carbon cycling by river damming. Nature communications, 8, 2017.

Maavara, T., Parsons, C. T., Ridenour, C., Stojanovic, S., Dürr, H. H., Powley, H. R., & Van Cappellen, P.: Global phosphorus retention by river damming. Proceedings of the National Academy of Sciences, 112(51), 15603-15608, 2015.

Mei, H., Wang, F., Yao, C., & Wang, B.: Diffusion Flux of Partial Pressure of Dissolved Carbon Dioxide in Wanan Reservoir in Spring. Environmental science, 32(1), 58-63. 2011.

Mendonça, R., Barros, N., Vidal, L. O., Pacheco, F., Kosten, S., & Roland, F.: Greenhouse Gas Emissions from Hydroelectric Reservoirs: What Knowledge Do We Have and What is Lacking? In G. Liu (Ed.), Greenhouse Gases - Emission, Measurement and Management, 2012a.

Mendonça, R., Kosten, S., Sobek, S., Barros, N., Cole, J. J., Tranvik, L., & Roland, F.: Hydroelectric carbon sequestration. Nature Geoscience, 5(12), 838-840, 2012b.

MEP. Ministry of Environmental Protection of People's Republic of China.: GB11893-89. In Water Quality-Determination of total phosphorous: Ammonium molybdate spectrophotometric method. Beijing: Standards Press of China, 1989.

MEP. Ministry of Environmental Protection of People's Republic of China.: HJ636-2012. In Water Quality - Determination of total nitrogen: Alkaline potassium persiflage digestion - UV spectrometric method. Beijing: Standards Press of China, 2012.

Mulholland, P. J., & Elwood, J. W.: The role of lake and reservoir sediments as sinks in the perturbed global carbon cycle. Tellus, 34(5), 490-499, 1982.

Pacheco, F., Soares, M., Assireu, A., Curtarelli, M., Roland, F., Abril, G., . . . Ometto, J.: River inflow and retention time affecting spatial heterogeneity of chlorophyll and water–air CO 2 fluxes in a tropical hydropower reservoir. Biogeosciences Discussions, 11(6), 8531-8568, 2014.

Pacheco, F. S., Roland, F., & Downing, J. A.: Eutrophication reverses whole-lake carbon budgets. Inland waters, 4(1), 41-48. doi:10.5268/IW-4.1.614, 2014.

Peng, X., Wang, B., Liu, C., Liu, X., & Wang, F.: Diurnal variations of pCO_2 in relation to environmental factors in the cascade reservoirs along the Wujiang River, China. Chinese Journal of Geochemistry, 31(1), 41-47, 2012.

Qu, B., Aho, K. S., Li, C., Kang, S., Sillanpää, M., Yan, F., & Raymond, P. A.: Greenhouse gases emissions in rivers of the Tibetan Plateau. Scientific reports, 7(1), 16573, 2017.

Ran, J., Lin, C., Guo, J., Chen, Y., & Jiang, T.: Spatial and temporal variation of carbon dioxide partial pressure over the Xiaojiang River backwater area of the Three Gorges Reservoir. Resource and Environment in the Yangtze Basin, 20(8), 976-982, 2011.

Ran LS, Li L, Tian M, Yang X, Yu R, Zhao J, Wang L, Lu XX.: Riverine CO2 emissions in the Wuding River catchment on the Loess Plateau: Environmental controls and dam impoundment impact. Journal of Geophysical Research: Biogeosciences 122 (6), 1439-1455, 2017.

RanLS., Tian M, Fang N, Wang S, Lu X.X., Yang X, Cho F.: Riverine carbon export in the arid to semiarid Wuding River catchment on the Chinese Loess Plateau. Biogeosciences 15 (12), 3857-3871, 2018.

Räsänen, T. A., Varis, O., Scherer, L., & Kummu, M.: Greenhouse gas emissions of hydropower in the Mekong River Basin. Environmental Research Letters, 2018.

Raymond, P. A., Hartmann, J., Lauerwald, R., Sobek, S., McDonald, C., Hoover, M., . . . Humborg, C.: Global carbon dioxide emissions from inland waters. Nature, 503(7476), 355-359, 2013.

Regnier, P., Andersson, A. J., Arndt, S., Arnosti, C., Borges, A. V., Dale, A. W., . . . Luyssaert, S.: Anthropogenic perturbation of the carbon fluxes from land to ocean. Nature Geoscience, 6(8), 597. doi:10.1038/ngeo1830, 2013.

Roland, F., Vidal, L., Pacheco, F., Barros, N., Assireu, A., Ometto, J. H. B., . . . Cole, J.: Variability of carbon dioxide flux from tropical (Cerrado) hydroelectric reservoirs. Aquatic Sciences, 72(3), 283-293. doi:10.1007/s00027-010-0140-0, 2010.

Rudd, J. W., Hecky, R., Harris, R., & Kelly, C. Are hydroelectric reservoirs significant sources of greenhouse gases, 1993.

Schelker, J., Singer, G. A., Ulseth, A. J., Hengsberger, S., & Battin, T. J.: CO_2 evasion from a steep, high gradient stream network: importance of seasonal and diurnal variation in aquatic pCO_2 and gas transfer. Limnology and Oceanography, 61(5), 1826-1838, 2016.

Senturk, F.: Hydraulics of dams and reservoirs. Highlands Ranch, Colo: Water Resources Publications, 1994.

Striegl, R. G., & Michmerhuizen, C. M.: Hydrologic influence on methane and carbon dioxide dynamics at two north-central Minnesota lakes. Limnology and Oceanography, 43(7), 1519-1529, 1998.

Summerfield, M. A. (1991). *Global geomorphology: an introduction to the study of landforms,* Harlow, Essex, England;New York;, Longman Scientific & Technical.

Tadonleke, R. D., Marty, J. m., & Planas, D.: Assessing factors underlying variation of CO_2 emissions in boreal lakes vs. reservoirs. FEMS microbiology ecology, 79(2), 282-297, 2012.

Teodoru, C. R., Prairie, Y. T. & Del Giorgio, P. A.: Spatial Heterogeneity of Surface CO2 Fluxes in a Newly Created Eastmain-1 Reservoir in Northern Quebec, Canada. Ecosystems, 14, 28-46, 2011.

Thornton, K. W., Kimmel, B. L., & Payne, F. E.: Reservoir limnology: ecological perspectives: John Wiley & Sons, 1990.

Tranvik, L. J., Downing, J. A., Cotner, J. B., Loiselle, S. A., Striegl, R. G., Ballatore, T. J., . . . Knoll, L. B.: Lakes and reservoirs as regulators of carbon cycling and climate. Limnology and Oceanography, 54(6), 2298-2314, 2009.

Tremblay, A., Varfalvy, L., Roehm, C., & Garneu, M.: Greenhouse gas emissions-fluxes and processes: Springer, 2005.

Varis, O., Kummu, M., Härkönen, S., & Huttunen, J. T.: Greenhouse gas emissions from reservoirs. In Impacts of Large Dams: A Global Assessment (pp. 69-94): Springer, 2012.

Vincent, L. S. L., Carol, A. K., Eric, D., John, W. M. R., & David, M. R.: Reservoir surfaces as sources of greenhouse gases to the atmosphere: A global estimate. Bioscience, 50(9), 766, 2000.

Vörösmarty, C. J., Meybeck, M., Fekete, B., Sharma, K., Green, P., & Syvitski, J. P.: Anthropogenic sediment retention: major global impact from registered river impoundments. Global and Planetary Change, 39(1), 169-190, 2003.

Wang, S., Wan, G., Liu, C., Yang, W., Zhu, Z., Xiao, H. & Tao, F.: Geochemical variation of CO2 and its atmospheric effect of lakes on the Yunnan-Guizhou Plateau (in Chinese). Quaternary Science, 23, 1, 2003.

Wang, B., Wang, Y., Wang, F., Liu, X., Liu, C.-Q., Guan, J., & Yu, Y.: Carbon dioxide emission from surface water in cascade reservoirs–river system on the Maotiao River, southwest of China. Atmospheric Environment, 45(23), 3827-3834. doi:10.1016/j.atmosenv.2011.04.014, 2011.

Xing, Y., Xie, P., Yang, H., Ni, L., Wang, Y., &Rong, K.: Methane and carbon dioxide fluxes from a shallow hypereutrophic subtropical Lake in China. Atmospheric Environment, 39(30), 5532-5540, 2005.

Xu, J., Zhang, P. & Wang, Y.: Land use and land cover in Lancang Watershed of Yunnan. Acta Botonica Yunnanica, 25,10, 2003.

Xu, Z.: Study of Carbon Dioxide and nitrous oxide emissions from Ecosystems of Different Elevations in a Typical Water Level Fluctuating Zone in Three Gorges Reservoir. Southwest University, 2013.

Yang, L., Lu, F., Wang, X., Duan, X., Song, W., Sun, B., . . . Zheng, F.: Surface methane emissions from different land use types during various water levels in three major drawdown areas of the Three Gorges Reservoir. Journal of Geophysical Research: Atmospheres (1984–2012), 117(D10), 2012.

Yang, M.: Spatial-temporal Variation of Greenhouse Gas Flux and Its Environmental Factors at Miyun Water Reservoir [D]. Beijing Forestry University, 2011.

Yang XK, Lu X.X., Ran LS.: Sustaining China's large rivers: River development policy, impacts, institutional issues and strategies for future improvement. Geoforum 69, 1-4, 2016.

Yang XK, Lu XX.: Drastic change in China's lakes and reservoirs over the past decades. Scientific reports 4, 6041, 2014.

Yu, Y., Wang, F., Wang, B., & Li, G.: Response of Dissolved Inorganic Carbon and Its Isotopic Spatial and Temporal Characteristics to the Earlier Reservoir Process: A Case Study on a New Reservoir (Hongjiadu) (in Chinese). Acta Mineralogica Sinica, 29(2), 268-274, 2009.

Zhao, Y., Wu, B. F., & Zeng, Y.: Spatial and temporal patterns of greenhouse gas emissions from Three Gorges Reservoir of China. Biogeosciences, 10(2), 1219-1230, 2013.

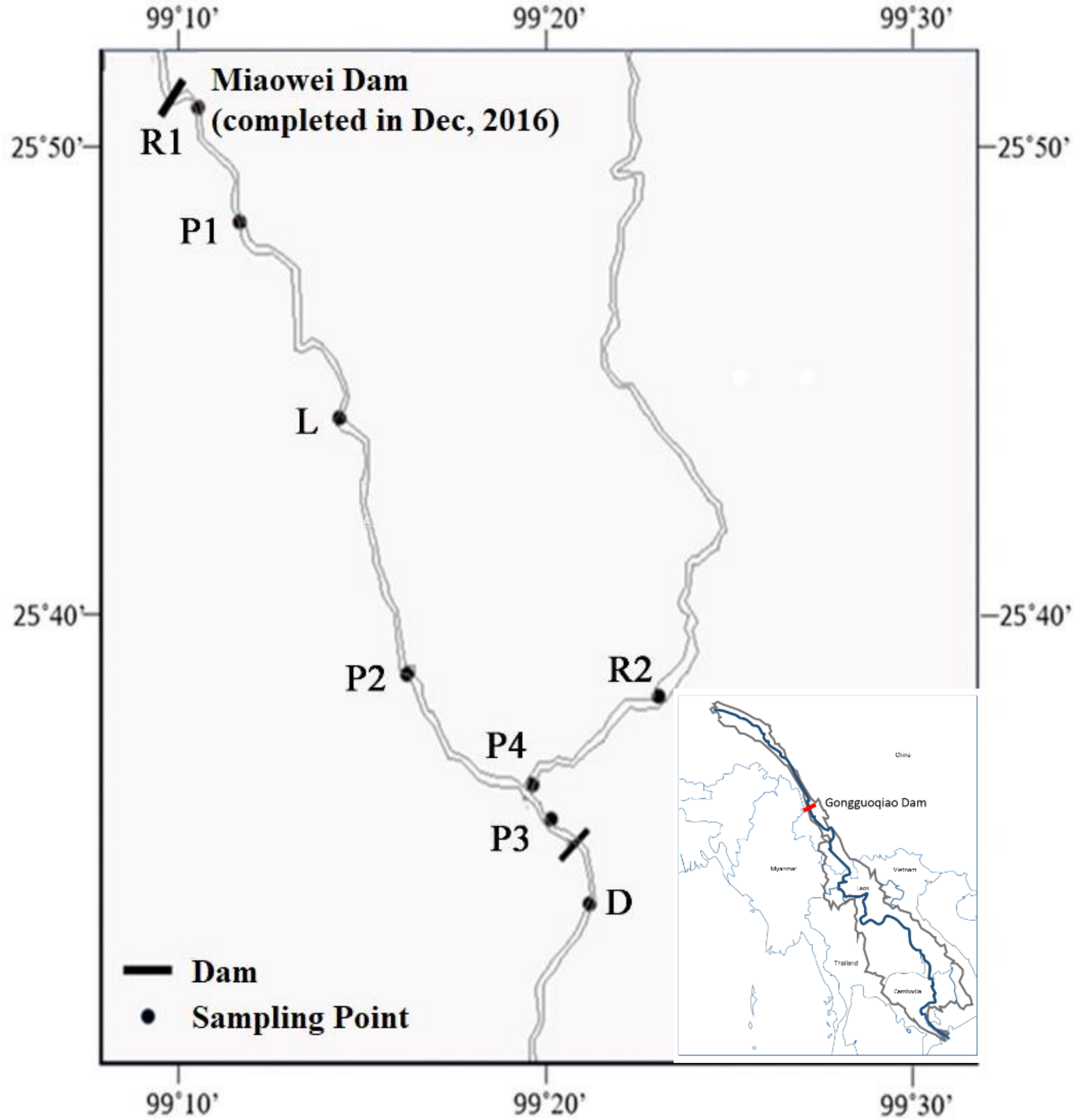

Figure 1 Sampling points in the Gongguoqiao Reservoir and its position within the Mekong River Basin. Point L1 is downstream the Miaowei Dam which was completed in Dec, 2016. Point R1 and R2 was in the river channel with flow velocity. Point P1, P2, P3 and P4 were in the reservoir without flow velocity. Point D was at the downstream of the reservoir. Point R2 and P4 were in the tributary the Bijiang River while all the other points were in the mainstemof Mekong River (or Lancang River).

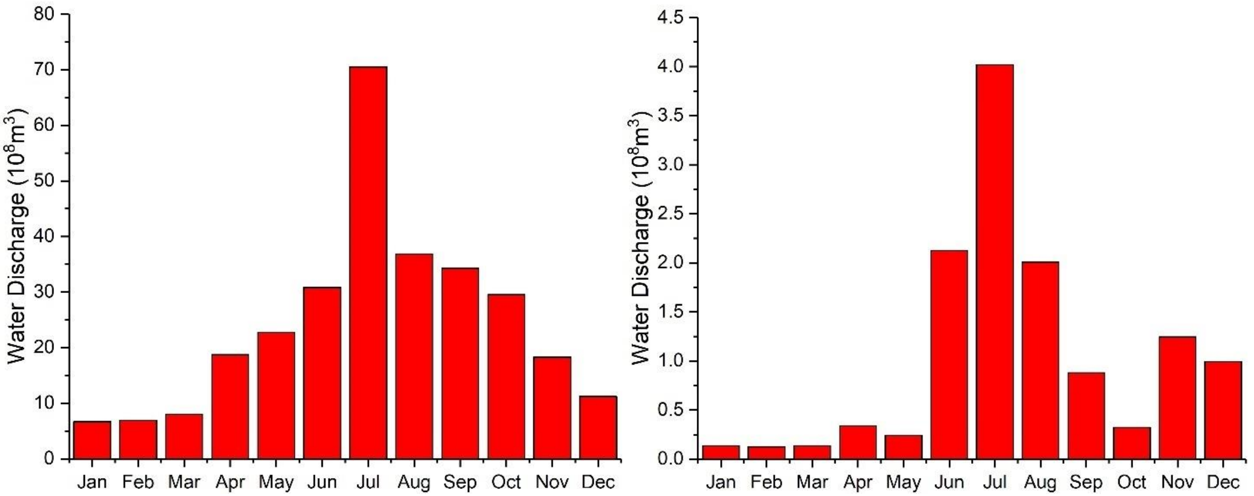

Figure 2 Monthly water discharge of the inflow at the mainstem (left panel) and the tributary (the Bijiang River, right panel) into the GGQ Reservoir. Notice that the inflow from the tributary was estimated with the instant water discharge (m3/s). The instant water discharge was measured at the same time as the sampling campaign at Point R2 at the Lanping or Yunlong Hydrological Gauging Station, which was about 30km away from Point R2.

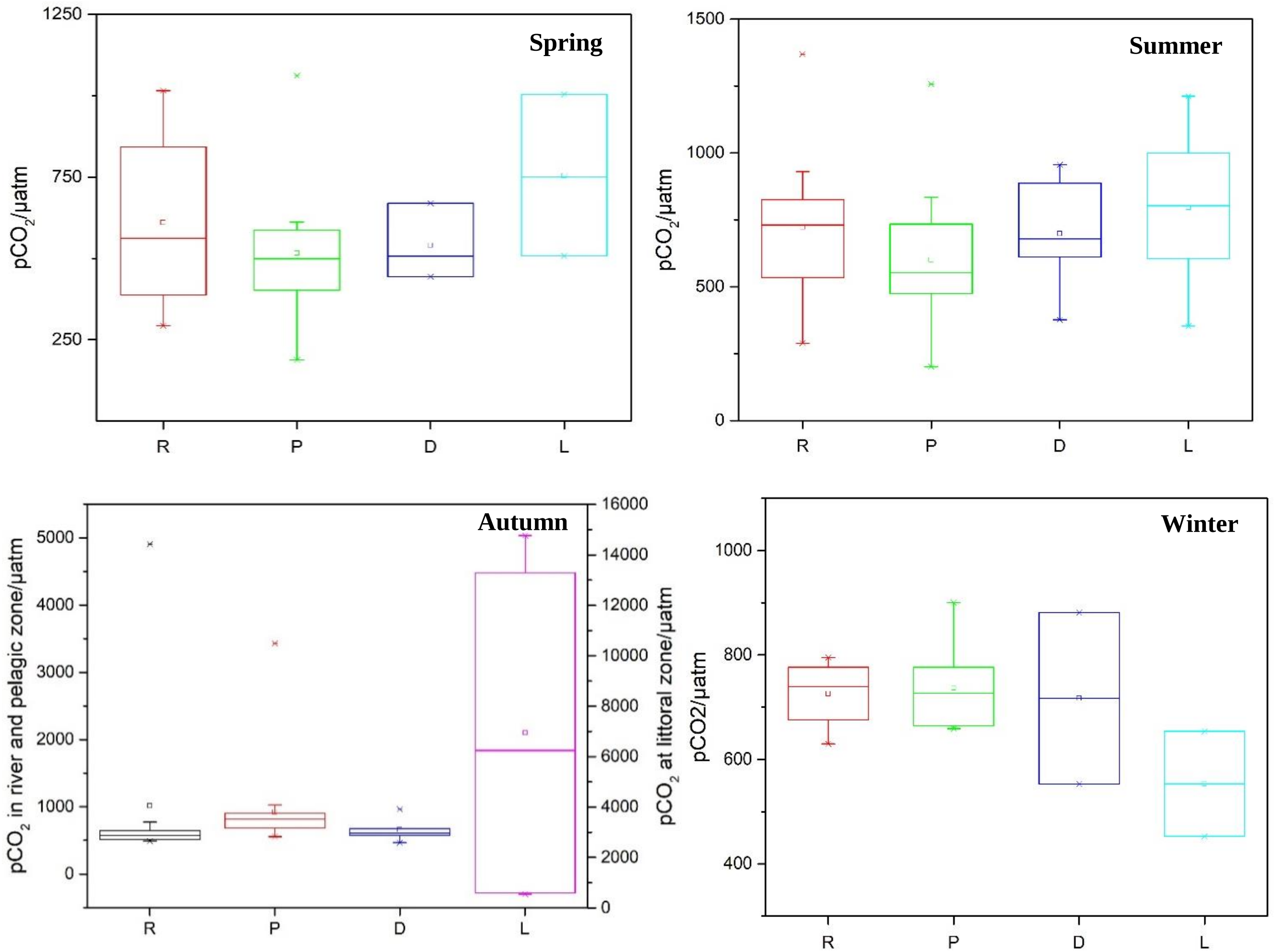

Figure 3 Box Plots of pCO_2 in the rivers (R), permanent flooded area of the reservoir (P), downstream (D) and littoral zone (L) in the four seasons. Notice that the scale of pCO_2 at the littoral zone in autumn was shown on the scale of right hand side. The vertical line indicates the 1.5 interquartile range. The points outside the range was considered outliers and are represented by little cross. Horizontal line refers to the median value while the little squares refers to the average. This could be applied to all the box plots below.

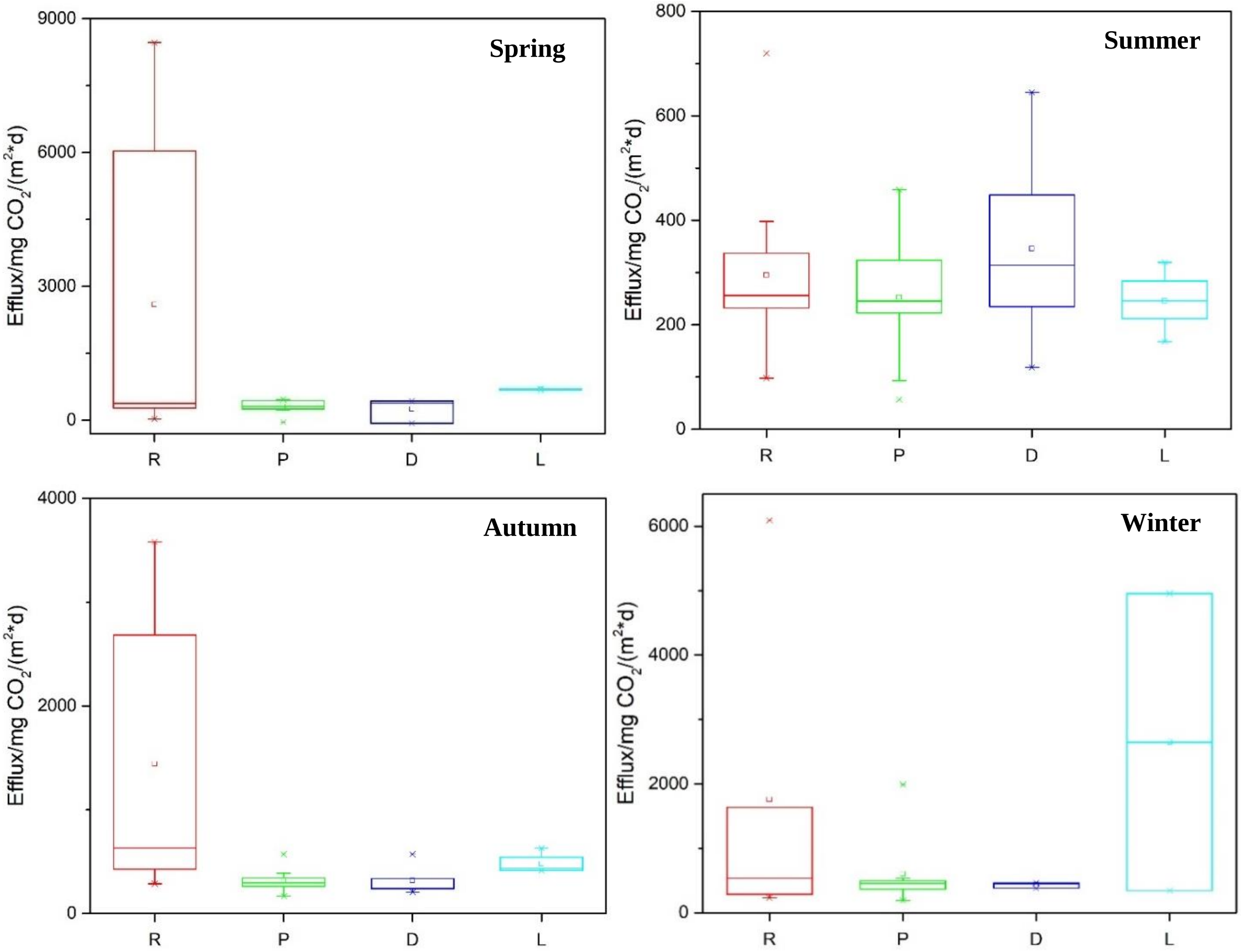

Figure 4 Box plots of the measured CO_2 effluxes in the four seasons. The legends are the same as Fig. 2.

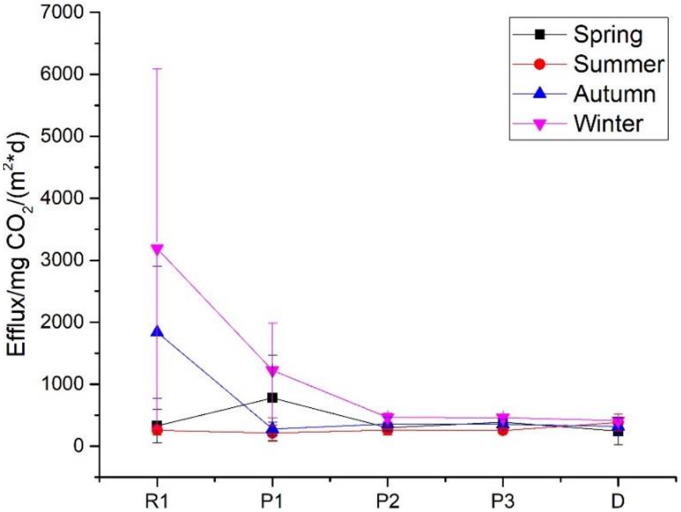

Figure 5 Longitudinal variation in effluxes along the mainstem in different seasons. The points and error bar refer to mean value and standard deviation respectively.

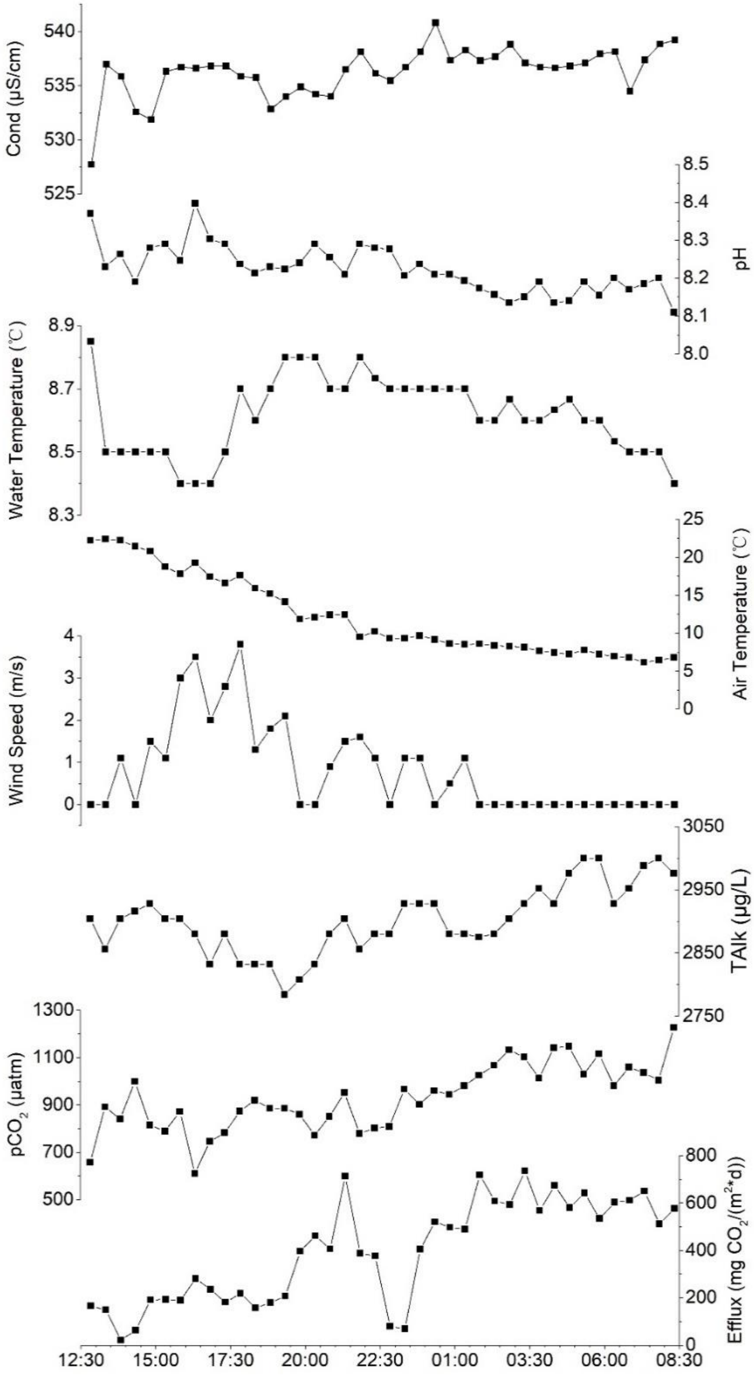

Figure6 Diurnal variation of the water environment (including conductivity, pH, water temperature and total alkalinity), atmospheric environment (air temperature and wind speed) pCO_2 and efflux.

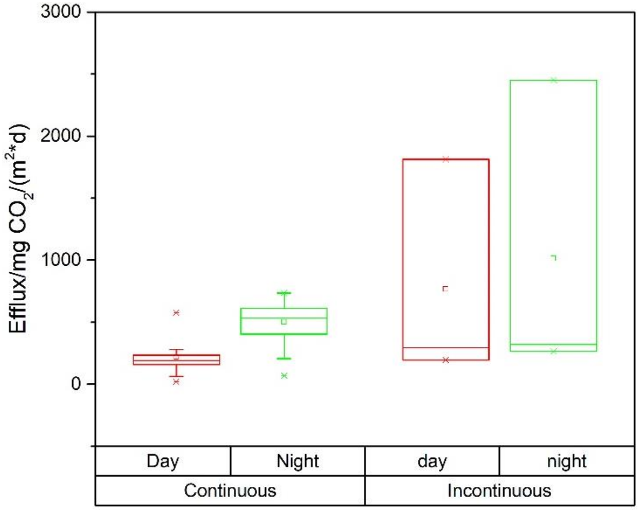

Figure7 Comparison in effluxes between daytime and night via continuous samples (left panel) and discontinuous samples (right panel)

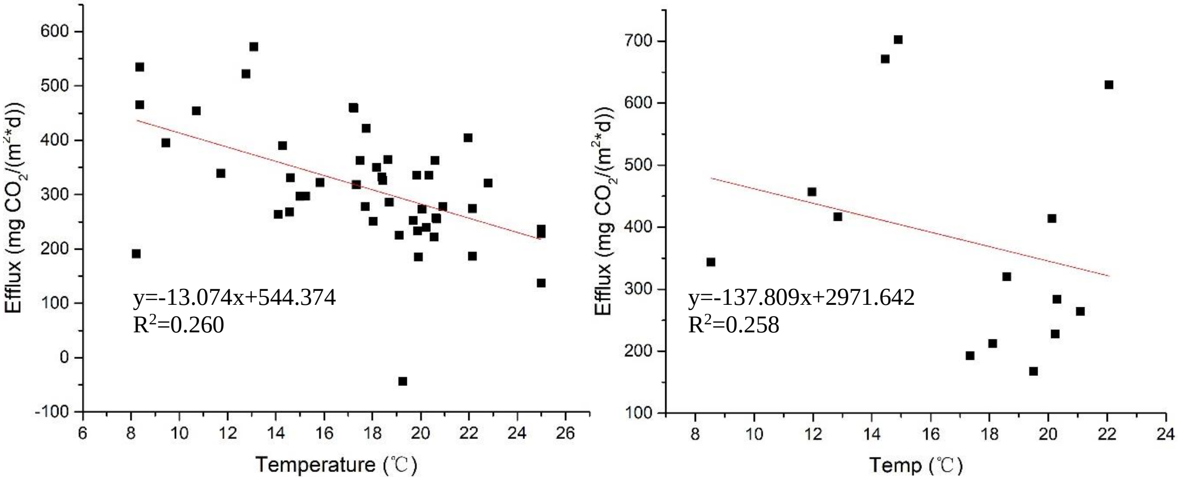

Figure 8 Negative correlations between water temperature and effluxes in the pelagic zone (left, $p<0.01$) and in the littoral zone (lower right, $p>0.05$). Notice that two extreme values were excluded out in the linear regression in the upper right panel

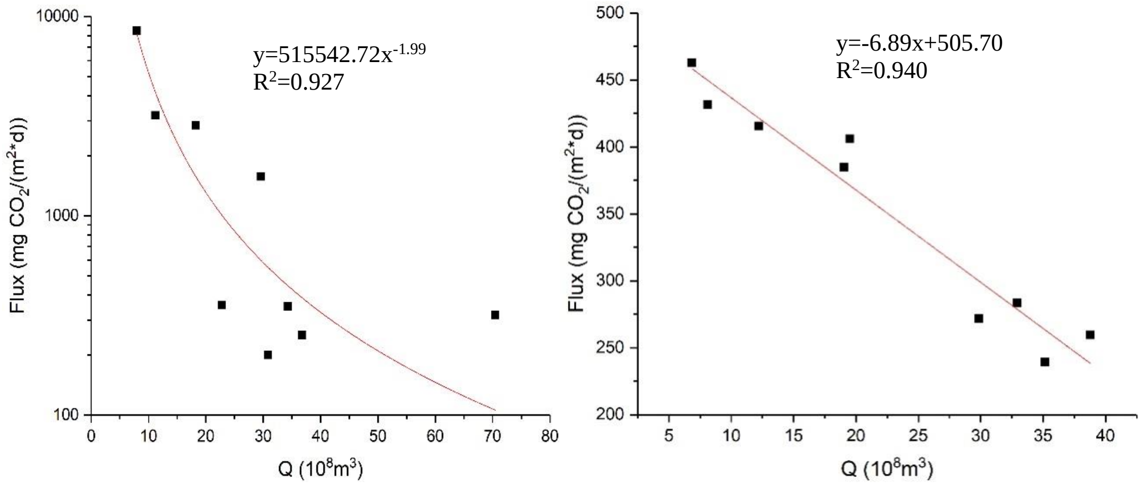

Figure 9 The negative correlation between water discharge and CO_2 efflux at the riverine inlet (R1, left panel, $p<0.01$) and outlet (D, right panel, $p<0.01$)

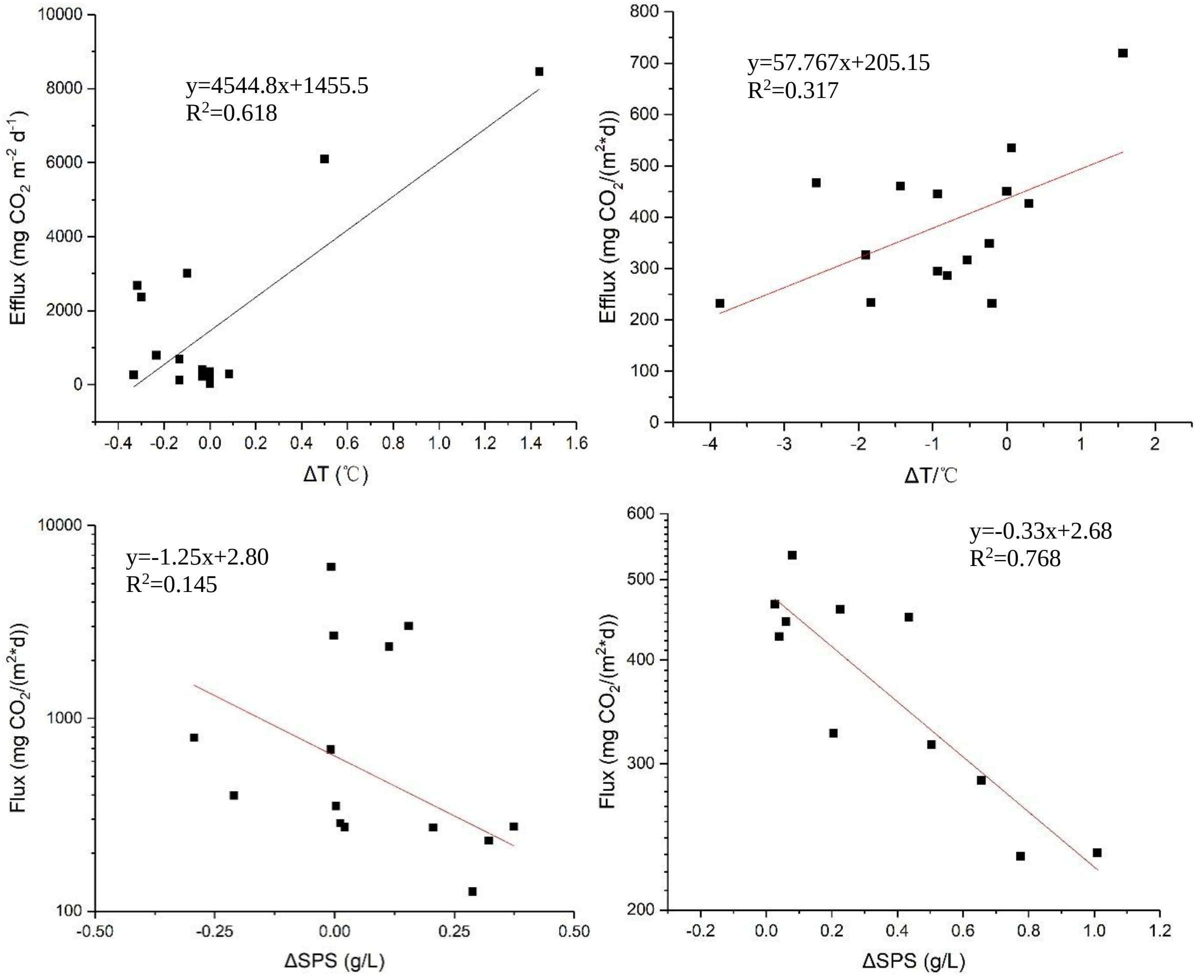

Figure 10 Positive correlations between water temperature gradient (TR1-P1 or TR2-P4) and measured effluxes at R1 (upper left, $p<0.01$) and R2 (upper right, $p<0.05$), and the negative correlations between SPS concentration gradient (SPS R1-P1 or SPS R2-P4) and measured effluxes at R1 (lower left, $p<0.01$) and R2 (lower right, $p<0.01$). The gradient in water temperature and SPS concentration reflects the difference of properties between inflow and receiving waterbody and determines the mixing mode. Colder and more turbid inflow has higher density than the receiving water and thus forms an underflow or subsurface flow (hyperpycnal flow). When the inflow was warmer clearer and lighter than the receiving waterbody, the inflow can form a surface flow (hypopycnal flow) and flow over the reservoir surface, releasing allochthonous carbon to the atmosphere.

Table 1 Mean temperature (Temp), pH, total alkalinity (Talk), conductivity (Cond), dissolved oxygen (DO), partial pressure of CO_2 (pCO_2), concentration of chlrophyll a (Chl a), concentration of total nitrogen (TN) and total phosphorous (TP) of sampling points

	Temp/℃	pH	Cond/μS/cm	DO/mg/L	Talk/μg/L	TN/mg/L	TP/mg/L	Chl a/mg/L	pCO_2/ppm
	Med (Min-Max)	Med (Min-Max)	Med (Min-Max)	Med (Min-Max)	Med (Min-Max)	Med (Min-Max)	Med (Min-Max)	Med (Min-Max)	Med (Min-Max)
R1	16.9(8.4-20.5)	8.40(7.47-8.61)	355.4(296.2-536.4)	8.93 (8.08-19.33)	2608(1696-3036)	0.51 (0.04-1.40)	0.12 (0.01-0.73)	0.99 (0.73-2.34)	572 (293-4902)
R2	19.2(8.3-21.1)	8.35(8.09-8.80)	295.0(159.8-437.7)	7.97 (4.61-20.16)	2508(1888-3456)	0.69 (0.20-4.47)	0.30 (0.01-1.65)	1.15 (0.75-2.09)	748 (289-1369)
P1	17.1(8.3-20.5)	8.38(7.63-8.86)	352.5(256.6-540.4)	8.81 (8.03-10.05)	2486(1712-2928)	0.51 (0.04-1.66)	0.04 (0.01-0.65)	1.01 (0.61-2.68)	621 (237-3427)
P2	17.8(8.4-25.0)	8.35(8.03-8.84)	330.5(214.2-537.2)	8.66 (7.94-9.32)	2338(1528-2928)	0.59 (0.04-2.30)	0.02 (0.01-0.52)	0.92 (0.75-1.68)	637 (201-1062)
P3	18.6(8.4-25.0)	8.28(8.05-8.49)	333.0(253.2-462.9)	8.30(7.49-8.83)	2262(1800-2772)	0.65 (0.04-1.59)	0.02 (0.01-0.49)	0.95 (0.62-1.84)	698 (448-1257)
P4	19.6(8.2-25.0)	8.34(8.08-8.77)	343.6 (259.4-494.2)	7.90(7.63-9.87)	2220(1888-2928)	0.79 (0.04-2.78)	0.02 (0.01-0.12)	0.99 (0.61-1.18)	747 (188-1183)
D	17.5(8.3-25.0)	8.37(8.17-8.62)	340.1 (266.0-529.2)	9.90(7.96-20.11)	2508(1784-3000)	0.52 (0.03-1.88)	0.02 (0.01-0.71)	0.99 (0.63-2.05)	615 (377-958)
L	18.1(8.5-22.1)	8.34(7.00-8.53)	357.7(275.4-539.4)	8.49(6.77-9.07)	2736(1928-4320)	0.61 (0.04-2.48)	0.02 (0.01-0.50)	0.98 (0.63-1.60)	750 (353-14764)